

^{57}Fe Mössbauer study of stoichiometric iron based superconductor $\text{CaKFe}_4\text{As}_4$: a comparison to KFe_2As_2 and CaFe_2As_2

Sergey L. Bud'ko*, Tai Kong¹, William R. Meier

Ames Laboratory US DOE and Department of Physics and Astronomy, Iowa State University, Ames, IA 50011, USA

Xiaoming Ma

Beijing National Laboratory for Condensed Matter Physics and Institute of Physics, Chinese Academy of Sciences, Beijing 100190, China.

Department of Physics, South University of Science and Technology of China, Shenzhen, Guangdong 518055, China

Paul C. Canfield

Ames Laboratory US DOE and Department of Physics and Astronomy, Iowa State University, Ames, IA 50011, USA

Abstract

^{57}Fe Mössbauer spectra at different temperatures between ~ 5 K and ~ 300 K were measured on an oriented mosaic of single crystals of $\text{CaKFe}_4\text{As}_4$. The data indicate that $\text{CaKFe}_4\text{As}_4$ is a well formed compound with narrow spectral lines, no traces of other, Fe - containing, secondary phases in the spectra and no static magnetic order. There is no discernible feature at the superconducting transition temperature in any of the hyperfine parameters. The temperature dependence of the quadrupole splitting approximately follows the empirical “ $T^{3/2}$ law”.

The hyperfine parameters of $\text{CaKFe}_4\text{As}_4$ are compared with those for KFe_2As_2 measured in this work, and the literature data for CaFe_2As_2 , and were found to be in between those for these two, ordered, 122 compounds, in agreement with the gross view of $\text{CaKFe}_4\text{As}_4$ as a structural analog of KFe_2As_2 and CaFe_2As_2 that has alternating Ca - and K - layers in the structure.

Keywords: superconductors, Mössbauer spectroscopy, hyperfine parameters

*Corresponding author

Email address: budko@ameslab.gov (Sergey L. Bud'ko)

¹currently at Department of Chemistry, Princeton University

1. Introduction

The discovery of iron-based superconductors [1] was followed by an outpouring of theoretical and experimental studies of those and related materials [2, 3, 4, 5]. Of these studies some were addressing specific details of the superconducting and the associated vortex state, whereas others were targeted comprehensive characterization of the general physical properties of iron-based superconductors and related materials. Mössbauer effect spectroscopy is widely accepted as one of the most sensitive techniques in terms of energy resolution. Historically, this technique has been applied to studies of superconductors for decades,[6] however its sensitivity specifically to the superconducting state is ambiguous. [7] It is quite natural that Mössbauer spectroscopy was widely used for studies of iron-based superconductors that naturally contain the common Mössbauer nuclide, ^{57}Fe , in the structure,[8, 9, 10, 11, 12]: no additional doping with ^{57}Fe (that can alter the properties of the material) is needed, and use of partially enriched Fe was required in only few, very specific cases. This technique was very successful in addressing the evolution of magnetic order, [13] structural phase transitions, [14] and phase purity [15, 16, 17] in these materials.

Recently, a new family of iron-based superconductors with rather high superconducting transition temperature, $T_c \sim 31 - 36$ K, has been discovered. [18] It was found that structurally ordered $\text{CaAFe}_4\text{As}_4$ (1144) compounds can be formed for $A = \text{K, Rb, Cs}$, and the key to the formation is the difference in ionic sizes between the Ca and the A ion. This family is not a $(\text{Ca}_{1-x}\text{A}_x)\text{Fe}_2\text{As}_2$ solid solution, where the Ca and A ions randomly occupy a single crystallographic site. [19] Along the c -axis, the Ca and A ions in this family form alternating planes that are separated by the Fe-As slabs (Fig. 1). In essence, the $\text{CaAFe}_4\text{As}_4$ structure is similar to the CaFe_2As_2 structure, just with layer by layer segregation of the Ca and A ions. The ordering of the layers causes a change of the space group from $I4/mmm$ to $P4/mmm$ and the Fe site in the 1144 structure has its point symmetry lowered to orthorhombic (from the tetragonal in the 122 structure). The 1144 structure was also found for $\text{SrAFe}_4\text{As}_4$ ($A = \text{Rb, Cs}$) [18] and $\text{EuAFe}_4\text{As}_4$ ($A = \text{Rb, Cs}$). [21, 22]

We were able to grow single-crystalline, single-phase samples of $\text{CaKFe}_4\text{As}_4$ and measure their anisotropic thermodynamic and transport properties. [23] The data indicated that $\text{CaKFe}_4\text{As}_4$ is an ordered stoichiometric superconductor with $T_c = 35$ K and no other phase transition for $1.8 \text{ K} \leq T \leq 300 \text{ K}$. It appeared to have properties very close to what is referred to as an optimally-doped, on a generalized phase diagram, iron-based superconductor. Being an ordered stoichiometric compound with a high value of T_c and a single crystallographic Fe site, $\text{CaKFe}_4\text{As}_4$ offers an exceptional opportunity to determine whether any of the hyperfine parameters exhibit an anomaly at superconducting transition. Additionally, this time with a local probe, we can evaluate the phase purity (in terms of possible Fe-containing phases) of the samples and the presence of static magnetic moment on the iron site. Furthermore, we can compare the temperature dependencies of the hyperfine parameters with those of the closely related compounds, CaFe_2As_2 and KFe_2As_2 .

In this work we will present results of the ^{57}Fe Mössbauer spectroscopy measurements between ~ 5 K and ~ 300 K on a mosaic of the oriented single crystals of $\text{CaKFe}_4\text{As}_4$ and will compare the results with similar sets of data for CaFe_2As_2 and KFe_2As_2 . Whereas there are available literature data for CaFe_2As_2 , [14, 24, 25] the published Mössbauer data for KFe_2As_2 apparently is limited to three temperature points [13] so we have chosen to collect a comprehensive set of data for KFe_2As_2 as a part of this work.

2. Experimental

$\text{CaKFe}_4\text{As}_4$ single crystals were grown by high temperature solution growth out of excess FeAs. The growth and basic physical properties are described in detail in Ref. [23]. The crystals were screened as described in Ref. [23] to avoid possible contaminations by CaFe_2As_2 and KFe_2As_2 minority phases. The superconducting transition in the $\text{CaKFe}_4\text{As}_4$ crystals used for the Mössbauer study was sharp with $T_c \sim 35$ K (Fig. 2).

KFe_2As_2 single crystals were also grown using a high-temperature solution growth technique. Starting elements were packed in an alumina frit-disc crucible set [26] with a molar ratio of K:Fe:As = 8:2:10. The crucible set together with the material were then welded in a Ta tube and sealed in a silica ampoule under a partial Ar atmosphere. A detailed drawing of such an assembly can be found in Ref [27]. The ampoule was slowly heated up to 920°C over ~ 40 hours, held at 920°C for 10 hours, quickly cooled to 850°C over 3 hours and then slowly cooled to 700°C over 3 days. At 700°C , the silica ampoule was inverted and decanted in a centrifuge. Remaining solution (primarily K-As) on the single crystals was rinsed off using ethanol. The resulting crystals had high residual resistivity ratio ($\rho(300\text{K})/\rho(5\text{K}) \sim 500$) and T_c values consistent with other high quality KFe_2As_2 crystals. [28, 29]

Mössbauer spectroscopy measurements were performed using a SEE Co. conventional, constant acceleration type spectrometer in transmission geometry with a $^{57}\text{Co}(\text{Rh})$ source kept at room temperature. Both for $\text{CaKFe}_4\text{As}_4$ and KFe_2As_2 the absorber was prepared as a mosaic of single crystals held on a paper disk by a small amount of Apiezon N grease. The gaps between the individual crystals were kept as small as possible. The mosaic had the c axis perpendicular to the disks and arbitrary in-plane orientation for each of the crystals. The c axis of the crystals in the mosaic was parallel to the Mössbauer γ beam. The absorber was cooled to a desired temperature using a Janis model SHI-850-5 closed cycle refrigerator (with vibration damping). The driver velocity was calibrated using an α -Fe foil, and all isomer shifts (IS) are quoted relative to the α -Fe foil at room temperature. The Mössbauer spectra were fitted using either the commercial software package MossWinn, [30] or the MossA package [31] with both analyses giving very similar results.

3. Results and Discussion

3.1. $\text{CaKFe}_4\text{As}_4$

A subset of Mössbauer spectra for $\text{CaKFe}_4\text{As}_4$, taken at different temperatures, is shown in Fig. 3. The absorption lines are asymmetric, suggesting that each spectrum is a quadrupole split doublet with rather small value of the quadrupole splitting, QS. There are no extra features observed, confirming that the samples are single phase. The results of fits to these data are shown in Fig. 4. The linewidth of the spectra (Fig. 4d - FWHM) varies between $\sim 0.23 - 0.26$ mm/s and is consistent with well ordered crystals. None of the hyperfine parameters has a detectable feature at $T_c = 35$ K that rises above the scattering of the data or the error bars.

Fig. 4a presents measured isomer shift (IS) which increases upon cooling. The isomer shift includes contributions from both the chemical shift and the second-order Doppler shift. The latter is known to increase convexly upon decreasing temperature, due to gradual depopulation of the excited phonon states, but should be constant at low temperature, because of the quantum mechanical zero-point motion. The chemical shift should not depend on temperature. The main contribution to the temperature dependence of the isomer shift then is considered to be from the second-order Doppler shift, and is usually described by the Debye model: [32]

$$IS(T) = IS(0) - \frac{9 k_B T}{2 M c} \left(\frac{T}{\Theta_D} \right)^3 \int_0^{\Theta_D/T} \frac{x^3 dx}{e^x - 1}, \quad (1)$$

where c is the velocity of light, M is the mass of the ^{57}Fe nucleus, and $IS(0)$ is the temperature-independent part. For the isomer shift data in Fig.4a Debye fit yields $\Theta_D = 370 \pm 9$ K.

The quadrupole splitting increases with decrease of temperature (Fig. 4b). The behavior can be described reasonably well with the empirical “ $T^{3/2}$ law” [33], $QS(T) = QS_0(1 - \beta T^{3/2})$, where $QS(T)$ is temperature dependent quadrupole splitting, QS_0 is its value at $T = 0$ K, β is a parameter that was found [33] to vary between 1×10^{-5} and $7 \times 10^{-5} \text{ K}^{-3/2}$. In our case the value of $\beta \approx 1.6 \times 10^{-5} \text{ K}^{-3/2}$ falls within the expected range.

Whereas the physics behind the “ $T^{3/2}$ law” is not fully understood (it is considered that that it originates from thermal vibrations of the lattice [34]), this relation describes reasonably well the temperature dependencies of QS observed in non-cubic metals. [33, 35, 36, 37]

The spectral area under the doublet increases on cooling (Fig. 4c). The temperature dependence of the spectral area can also be fitted with the Debye model [32]:

$$f = \exp \left\{ \frac{-3E_\gamma^2}{k_B \Theta_D M c^2} \left[\frac{1}{4} + \left(\frac{T}{\Theta_D} \right)^2 \int_0^{\Theta_D/T} \frac{x dx}{e^x - 1} \right] \right\}, \quad (2)$$

where f is the recoilless fraction, which is proportional to the area for a thin sample and E_γ is the γ -ray energy. The estimate of the Debye temperature from the fit gives $\Theta_D = 247 \pm 1$ K, a value that is about 125 K less than the value estimated by temperature dependence of IS . Although part of this discrepancy could be due to deviations from the thin absorber conditions of the measurements, it should be mentioned that similar differences were found earlier in studies of $\text{Lu}_2\text{Fe}_3\text{Si}_5$, $\text{FeSe}_{0.5}\text{Te}_{0.5}$ and ^{57}Fe doped $\text{YBa}_2\text{Cu}_3\text{O}_{6.8}$ compounds. [7, 38, 39] This discrepancy may be explained by the fact the area reflects the average mean-square displacements, whereas IS is related to the mean-square velocity of the Mössbauer atom. Both quantities may respond in a different way to lattice anharmonicities.

The temperature dependent linewidth of the spectra is shown in Fig. 4d. Overall the linewidth increases by a few percent on cooling from room temperature to the base temperature. The observed spectral lines for $\text{CaKFe}_4\text{As}_4$ are somewhat narrower than those in CaFe_2As_2 [14, 24] and KFe_2As_2 (see below) single crystal measurements, and measurably sharper than the Mössbauer spectra lines in the substituted $\text{Ca}(\text{Fe}_{0.965}\text{Co}_{0.035})_2\text{As}_2$ [40] that vary in the range of 0.28 - 0.35 mm/s between room temperature and 5 K. This suggests that $\text{CaKFe}_4\text{As}_4$ crystals used in this work are well ordered.

In the AFe_2As_2 ($A = \text{Ba, Sr, Ca, Cs, Rb, K}$) compounds the point symmetry ($-4m2$) and the location of the Fe site in the crystal structure constrains the principal axis of the local electric field gradient tensor to the c -crystalline axis; as a result, a doublet lines intensity ratio of 3:1 is expected for the mosaic with the c - axis parallel to the γ - beam. Per contra, in the $\text{CaKFe}_4\text{As}_4$ the point symmetry ($2mm$) of the Fe site formally does not impose such constrain [18] and some deviation from the 3 : 1 ratio is expected. This said, the Fe - As1 and Fe - As2 bond lengths as well as As1 - Fe - As1 and As2 - Fe - As2 bonds angles are very similar and we would not expect significant difference from the AFe_2As_2 case. The experimentally observed room temperature ratio is $\sim 2.3 : 1$, and it decreases to $\sim 1.9 : 1$ at the base temperature (Fig. 4e). Very similar deviations from the 3:1 ratio were observed for measurements on CaFe_2As_2 single crystals [14, 25, 41] and several possible reasons for the doublet lines intensity ratio being different from 3:1 were discussed, e.g. a thick absorber conditions of the measurements and some misorientation of the crystals that form the absorber mosaic. The same arguments, in addition to the different point group symmetry for Fe, are probably appropriate when considering the $\text{CaKFe}_4\text{As}_4$ results.

3.2. KFe_2As_2

Fig. 5 shows a subset of Mössbauer spectra of KFe_2As_2 taken at different temperatures. The asymmetry is even less pronounced than in the $\text{CaKFe}_4\text{As}_4$ spectra above. Still, good fit of the data can be obtained by using a doublet with small quadrupole splitting. For KFe_2As_2 , similarly to the $\text{CaKFe}_4\text{As}_4$, the principal axis of the local electric field gradient tensor should be parallel to the c -crystalline axis and the doublet lines intensity ratio of 3:1 is expected. If the fits are performed with this ratio left as a free parameter, within the

error bars the expected $A1/A2 = 3$ is obtained for all temperatures. To reduce the uncertainty in particular, in the small values of quadrupole splitting, we repeated the fits with fixed the $A1/A2 = 3$ parameter. The results are shown in Fig. 6. In comparison with the data obtained on powders at three different temperatures, [13], our linewidth is smaller and values of the isomer shift are bigger, although the overall changes, ΔIS , from room temperature to the base temperatures are very similar.

The linewidth and its temperature dependence (Fig. 6d) are similar to those observed for $\text{CaKFe}_4\text{As}_4$. The temperature dependent isomer shift and spectral area are well fit using the Debye model, as described above (Fig. 6a,c). These fits yield the values of Θ_D of 474 ± 20 K (from $IS(T)$) and 325 ± 7 K (from temperature dependent spectral area). In comparison with $\text{CaKFe}_4\text{As}_4$, the Debye temperatures are higher in KFe_2As_2 , suggesting that the lattice is stiffer.

The values of quadrupole splitting (Fig. 6b) for KFe_2As_2 are significantly smaller than those for $\text{CaKFe}_4\text{As}_4$, moreover QS decreases with decrease of temperature, as opposed to increase following the “ $T^{3/2}$ law” in $\text{CaKFe}_4\text{As}_4$. Although the theoretical foundations of the empirical “ $T^{3/2}$ law” are not well understood and different (constant, vs $T^{3/2}$) $QS(T)$ behavior has been observed for related ($\text{Ce}_{0.35}\text{FeCo}_3\text{Sb}_{12}$ vs $\text{Ce}_{0.98}\text{Fe}_4\text{Sb}_{12}$) materials,[36] this observation in iron-arsenides calls for further studies.

3.3. Comparison of $\text{CaKFe}_4\text{As}_4$, KFe_2As_2 , and CaFe_2As_2

Since, naively speaking, the $\text{CaKFe}_4\text{As}_4$ structure can be viewed as being constructed from the alternating slabs of CaFe_2As_2 and KFe_2As_2 structures, it would be of use to compare the ^{57}Fe hyperfine parameters of these three compounds. Whereas $\text{CaKFe}_4\text{As}_4$ and KFe_2As_2 do not exhibit static magnetic order or a structural transition below room temperature, CaFe_2As_2 is known to be more complex. CaFe_2As_2 grown out of Sn flux [42] exhibits concomitant structural (high temperature tetragonal to low temperature orthorhombic) and magnetic (paramagnetic to low temperature antiferromagnetic) transitions at ≈ 173 K. [42, 43]. In the following we will refer to this sample as CaFe_2As_2 - AFM and use the hyperfine parameters from the single crystal work, Ref. [24]. In the CaFe_2As_2 sample grown out of FeAs flux, by judicious choice of annealing / quenching conditions [41] we can stabilize low temperature ambient pressure collapsed tetragonal (cT) phase with the structural transition at ≈ 90 K. This sample will be referred in the following as CaFe_2As_2 - cT, and the hyperfine parameters from the ref. [14] will be used.

The hyperfine parameters for the $\text{CaKFe}_4\text{As}_4$, KFe_2As_2 , and CaFe_2As_2 compounds at room temperature and the base temperature are summarized in the Table 1. The temperature dependencies are presented in the plots below. The spectral linewidths of these compounds are very similar (Fig. 7). The smallest one is observed for $\text{CaKFe}_4\text{As}_4$, possibly pointing out to very well formed crystals. The isomer shift in $\text{CaKFe}_4\text{As}_4$ (Fig. 8). has values in between those for KFe_2As_2 and CaFe_2As_2 . Note that the $IS(T)$ for CaFe_2As_2 - cT has a small but distinct feature associated with the cT transition. Similarly, the quadrupole splitting of $\text{CaKFe}_4\text{As}_4$ (Fig. 9) has values in between the values for two other

compounds. Both, CaFe_2As_2 - cT and CaFe_2As_2 - AFM have clear features associated with the cT and the structural / AFM transitions, respectively. It is curious (although it might be a mere coincidence) that $QS(T)$ of $\text{CaKFe}_4\text{As}_4$ and the absolute values of $QS(T)$ of CaFe_2As_2 - AFM below the structural / AFM transition are laying basically on top of each other. As for the overall temperature behavior, it appears that only for KFe_2As_2 $QS(T)$ decreases with decrease of temperature. It would be of interest to see if different temperature dependences are observed in quadrupole frequencies when measured in these materials by ^{75}As nuclear magnetic resonance. As for normalized (at the respective base temperatures) spectral areas (Fig. ??), again, CaFe_2As_2 - cT and CaFe_2As_2 - AFM have anomalies at the corresponding transitions. The data points for $\text{CaKFe}_4\text{As}_4$, CaFe_2As_2 - cT and CaFe_2As_2 - AFM (below the structural / AFM transition) are, grossly speaking, following the same temperature dependence. The data for KFe_2As_2 are somewhat distinct, pointing either to stiffer phonon spectrum or some additional contribution to the temperature dependence of the spectral area in this compound.

4. Summary

The measurements of ^{57}Fe Mössbauer spectra on oriented mosaics of single crystals of $\text{CaKFe}_4\text{As}_4$ and KFe_2As_2 were performed and the results were compared with the literature data for CaFe_2As_2 .

$\text{CaKFe}_4\text{As}_4$ can be characterized as a well formed compound with narrow spectral lines and no traces of other, Fe - containing, secondary phases in the spectra. There is no feature in hyperfine parameters at T_c and no indication of static magnetic order. The values of the ^{57}Fe hyperfine parameters of $\text{CaKFe}_4\text{As}_4$ are in between those for KFe_2As_2 and CaFe_2As_2 , in agreement with the gross view of $\text{CaKFe}_4\text{As}_4$ as a structural analog of KFe_2As_2 and CaFe_2As_2 with alternating Ca - and K - layers in the structure. The $QS(T)$ generally follows the empirical “ $T^{3/2}$ law”. Debye fits of the temperature dependencies of the isomer shift and the spectral area yield the Debye temperatures of ~ 370 K and ~ 247 K respectively.

KFe_2As_2 has smaller quadrupole splitting and isomer shift in comparison with $\text{CaKFe}_4\text{As}_4$ and CaFe_2As_2 . Its QS decreases slightly on cooling that differs from the generic behavior observed in many non-cubic metals. The Debye temperatures evaluated from the temperature dependent IS and spectral area are ~ 474 K and ~ 325 K respectively, these values being ~ 100 K higher than those for $\text{CaKFe}_4\text{As}_4$.

Acknowledgments

This work was supported by the U.S. Department of Energy, Office of Basic Energy Science, Division of Materials Sciences and Engineering. The research was performed at the Ames Laboratory. Ames Laboratory is operated for the

U.S. Department of Energy by Iowa State University under Contract No. DE-AC02-07CH11358. In addition, W. R. M. was supported by the Gordon and Betty Moore Foundations EPiQS Initiative through Grant GBMF4411.

References

References

- [1] Y. Kamihara, T. Watanabe, M. Hirano, H. Hosono, *J. Am. Chem. Soc.* 130 (2008) 3296.
- [2] P. C. Canfield and S. L. Bud'ko, *Annu. Rev. Condens. Matter Phys.* 1 (2010) 27.
- [3] D. C. Johnston, *Adv. Phys.* 59 (2010) 803.
- [4] G. R. Stewart, *Rev. Mod. Phys.* 83 (2011) 1589.
- [5] N.-L. Wang, H. Hosono and P.-C. Dai (eds.), *Iron-based Superconductors. Materials, Properties and Mechanisms* (Pan Stanford Publishing, Boca Raton, FL, 2012).
- [6] P. P. Craig, R. D. Taylor, and D. E. Nagle, *Nuovo Cim.* 22 (1961) 402.
- [7] Xiaoming Ma, Sheng Ran, Hua Pang, Fashen Li, Paul C. Canfield, and Sergey L. Bud'ko, *J. Phys. Chem. Solids* 83 (2015) 58.
- [8] Israel Nowik, Israel Felner, *Physica C* 469 (2009) 485.
- [9] M. G. Kozin, I. L. Romashkina, *Izv. Ros. Akad. Nauk, Ser. Fiz.* 74 (2010) 360 [*Bull. Rus. Acad. Sci.: Physics* 74 (2010) 330].
- [10] A. Błachowski, K. Ruebenbauer, and J. Żukrowski, *The Annales UMCS, Sectio AAA - Physica* 66 (2011) 125.
- [11] Amar Nath and Airat Khasanov, in: *Mössbauer Spectroscopy: Applications in Chemistry, Biology, and Nanotechnology*, edited by Virender K. Sharma, Gostar Klingelhofer, and Tetsuaki Nishida (John Wiley & Sons, Inc., Hoboken, NJ, 2013), p. 535.
- [12] A. K. Jasek, K. Komędera, A. Błachowski, K. Ruebenbauer, J. Żukrowski, Z. Bukowski, and J. Karpinski, *Philos. Mag.* 95 (2015) 493.
- [13] Marianne Rotter, Marcus Tegel, Inga Schellenberg, Falko M. Schappacher, Rainer Pöttgen, Joachim Deisenhofer, Axel Günther, Florian Schrettle, Alois Loidl, and Dirk Johrendt, *New J. Phys.* 11 (2009) 125014.
- [14] Sergey L. Bud'ko, Xiaoming Ma, Milan Tomić, Sheng Ran, Roser Valentí, and Paul C. Canfield, *Phys. Rev. B* 93 (2016) 024516.

- [15] Israel Felner, Israel Nowik, Bing Lv, Joshua H. Tapp, Zhongjia Tang, and Arnold M. Guloy, *Hyperfine Int.* 191 (2009) 61.
- [16] D. H. Ryan, W. N. Rowan-Weetaluktuk, J. M. Cadogan, R. Hu, W. E. Straszheim, S. L. Bud'ko, and P. C. Canfield, *Phys. Rev. B* 83 (2011) 104526.
- [17] Vadim Ksenofontov, Gerhard Wortmann, Sergey A. Medvedev, Vladimir Tsurkan, Joachim Deisenhofer, Alois Loidl, and Claudia Felser, *Phys. Rev. B* 84 (2011) 180508.
- [18] Akira Iyo, Kenji Kawashima, Tatsuya Kinjo, Taichiro Nishio, Shigeyuki Ishida, Hiroshi Fujihisa, Yoshito Gotoh, Kunihiro Kihou, Hiroshi Eisaki, and Yoshiyuki Yoshida, *J. Amer. Chem. Soc.* 138 (2016) 3410.
- [19] D. M. Wang, X. C. Shangguan, J. B. He, L. X. Zhao, Y. J. Long, P. P. Wang, and L. Wang, *J. Supercond. Nov. Magn.* 26 (2013) 2121.
- [20] K. Momma and F. Izumi, *J. Appl. Crystallogr.*, 44 (2011) 1272.
- [21] Yi Liu, Ya-Bin Liu, Zhang-Tu Tang, Hao Jiang, Zhi-Cheng Wang, Abduweli Ablimit, Wen-He Jiao, Qian Tao, Chun-Mu Feng, Zhu-An Xu, and Guang-Han Cao, *Phys. Rev. B* 93 (2016) 214503.
- [22] Yi Liu, Ya-Bin Liu, Qian Chen, Zhang-Tu Tang, Wen-He Jiao, Qian Tao, Zhu-An Xu, Guang-Han Cao, *Science Bulletin* 61 (2016) 1213.
- [23] W. R. Meier, T. Kong, U. S. Kaluarachchi, V. Taufour, N. H. Jo, G. Drachuck, A. E. Böhmer, S. M. Saunders, A. Sapkota, A. Kreyssig, M. A. Tanatar, R. Prozorov, A. I. Goldman, Fedor F. Balakirev, Alex Gurevich, S. L. Bud'ko, and P. C. Canfield, *Phys. Rev. B* 94 (2016) 064501.
- [24] Xiaoming Ma, Sheng Ran, Paul C. Canfield, Sergey L. Bud'ko, *J. Alloys Compd* 657 (2016) 379.
- [25] M. Alzamora, J. Munevar, E. Baggio-Saitovitch, S. L. Bud'ko, Ni Ni, P. C. Canfield, and D. R. Sánchez, *J. Phys.: Cond. Mat.* 23 (2011) 145701.
- [26] Paul C. Canfield, Tai Kong, Udhara S. Kaluarachchi, and Na Hyun Jo, *Philos. Mag.* 96 (2016) 84.
- [27] Tai Kong, Sergey L. Bud'ko, and Paul C. Canfield, *Phys. Rev. B* 91 (2015) 020507.
- [28] Kunihiro Kihou, Taku Saito, Shigeyuki Ishida, Masamichi Nakajima, Yasuhide Tomioka, Hideto Fukazawa, Yoh Kohori, Toshimitsu Ito, Shin-ichi Uchida, Akira Iyo, Chul-Ho Lee, and Hiroshi Eisaki, *J. Phys. Soc. Jpn.* 79 (2010) 124713.
- [29] Yong Liu, M. A. Tanatar, V. G. Kogan, Hyunsoo Kim, T. A. Lograsso, and R. Prozorov, *Phys. Rev. B* 87 (2013) 134513.

- [30] Z. Klenczár, MossWinn 4.0 Manual (2016).
- [31] C. Prescher, C. McCammon and L. Dubrovinsky, *J. Appl. Cryst.* 45 (2012) 329.
- [32] Philipp Gütlich, Eckhard Bill, and Alfred X. Trautwein, *Mössbauer Spectroscopy and Transition Metal Chemistry. Fundamentals and Applications*, Springer-Verlag, Berlin, Heidelberg, (2011).
- [33] R. Vianden, *Hyperfine Int.* 15/16 (1983) 189.
- [34] K. Nishiyama, F. Dimmling, Th. Kornrumpf, and D. Riegel, *Phys. Rev. Lett.* 37 (1976) 357.
- [35] H. C. Verma and G. N. Rao, *Hyperfine Int.* 15/16 (1983) 207.
- [36] Gary J. Long, Dimitri Hutot, Fernande Grandjean, Donald T. Morelli, and Gregory P. Meisner, *Phys. Rev. B* 60 (1999) 7410.
- [37] Ichiro Tamura, Tsuyoshi Ikeno, Toshio Mizushima, and Yosikazu Isikawa, *J. Phys. Soc. Jpn.* 81 (2012) 074703.
- [38] J. Lindén, J.-P. Libäck, M. Karppinen, E.-L. Rautama, H. Yamauchi, *Solid State Commun.* 151 (2011), 130.
- [39] V.M. Cherepanov, M.A. Chuev, E. Yu. Tsymbal, Ch. Sauer, W. Zinn, S.A. Ivanov, V.V. Zhurov, *Solid State Commun.* 93 (1995) 921.
- [40] A. E. Böhmer, A. Sapkota, A. Kreyssig, S. L. Bud'ko, G. Drachuck, S. M. Saunders, A. I. Goldman, P. C. Canfield, preprint, arXiv:1612.07341 (2016), *Phys. Rev. Lett.* - in press.
- [41] S. Ran, S. L. Bud'ko, D. K. Pratt, A. Kreyssig, M. G. Kim, M. J. Kramer, D. H. Ryan, W. N. Rowan-Weetaluktuk, Y. Furukawa, B. Roy, A. I. Goldman, and P. C. Canfield, *Phys. Rev. B* 83 (2011) 144517.
- [42] N. Ni, S. Nandi, A. Kreyssig, A. I. Goldman, E. D. Mun, S. L. Bud'ko, and P. C. Canfield, *Phys. Rev. B* 78 (2008) 014523.
- [43] A. I. Goldman, D. N. Argyriou, B. Ouladdiaf, T. Chatterji, A. Kreyssig, S. Nandi, N. Ni, S. L. Bud'ko, P. C. Canfield, and R. J. McQueeney, *Phys. Rev. B* 78 (2008) 100506.

Table 1: Hyperfine parameters of $\text{CaKFe}_4\text{As}_4$, KFe_2As_2 , and CaFe_2As_2 at room temperature and base temperature

sample	T (K)	IS (mm/s)	QS (mm/s)	FWHM (mm/s)	Ref.
$\text{CaKFe}_4\text{As}_4$	297	0.372(2)	0.140(3)	0.232(3)	this work
	4.8	0.511(2)	0.149(2)	0.251(3)	this work
KFe_2As_2	296	0.311(1)	0.113(4)	0.244(3)	this work
	4.7	0.431(3)	0.05(1)	0.265(4)	this work
CaFe_2As_2 - AFM	296	0.448(2)	0.202(2)	0.254(3)	[24]
	4.6	0.5708(7)	-0.159(1)	0.280(2)	[24]
CaFe_2As_2 - cT	293	0.430(2)	0.225(3)	0.269(3)	[14]
	4.6	0.5902(5)	0.2758(7)	0.274(1)	[14]

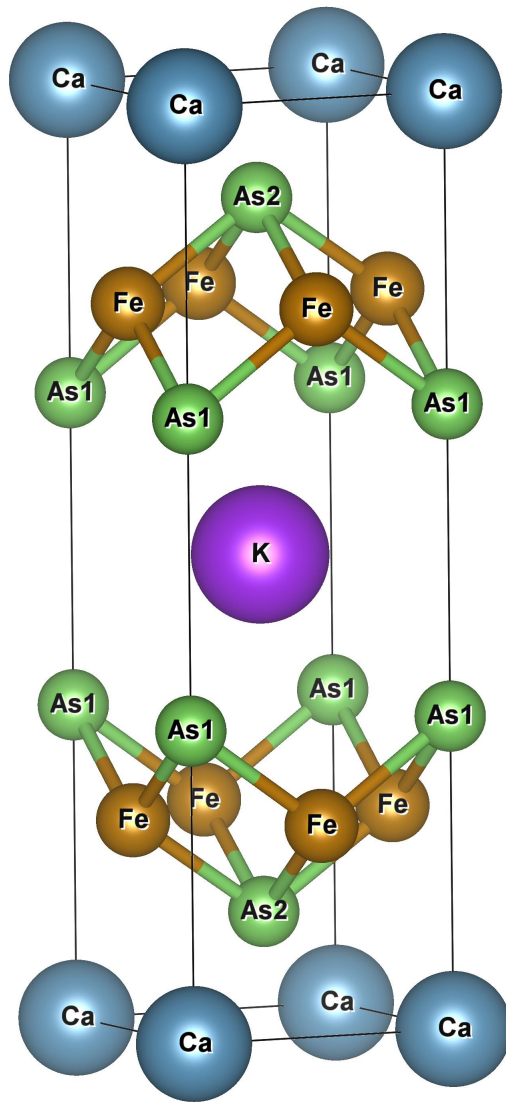


Figure 1: (Color online) Crystal structure of $\text{CaKFe}_4\text{As}_4$ sketched using VESTA [20].

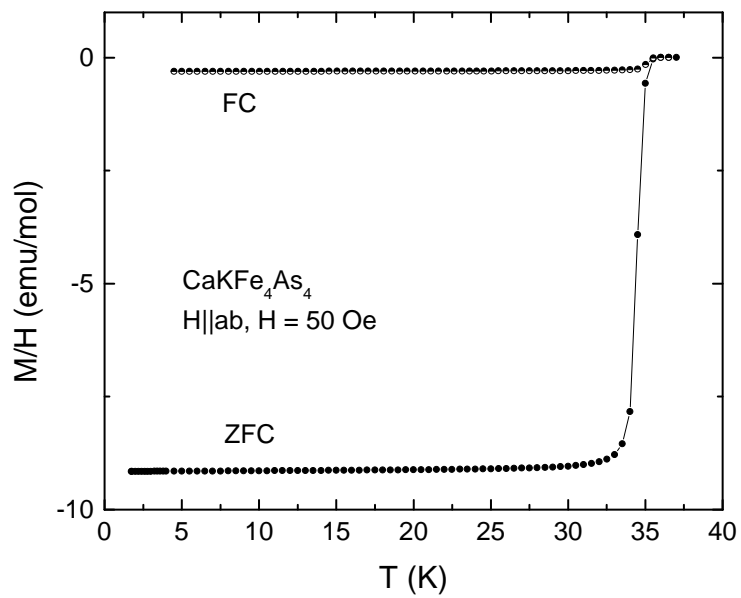


Figure 2: Low field, low temperature zero-field-cooled (ZFC) and field cooled (FC) DC susceptibility of one of the $\text{CaKFe}_4\text{As}_4$ crystals used in the mosaic for Mössbauer measurements.

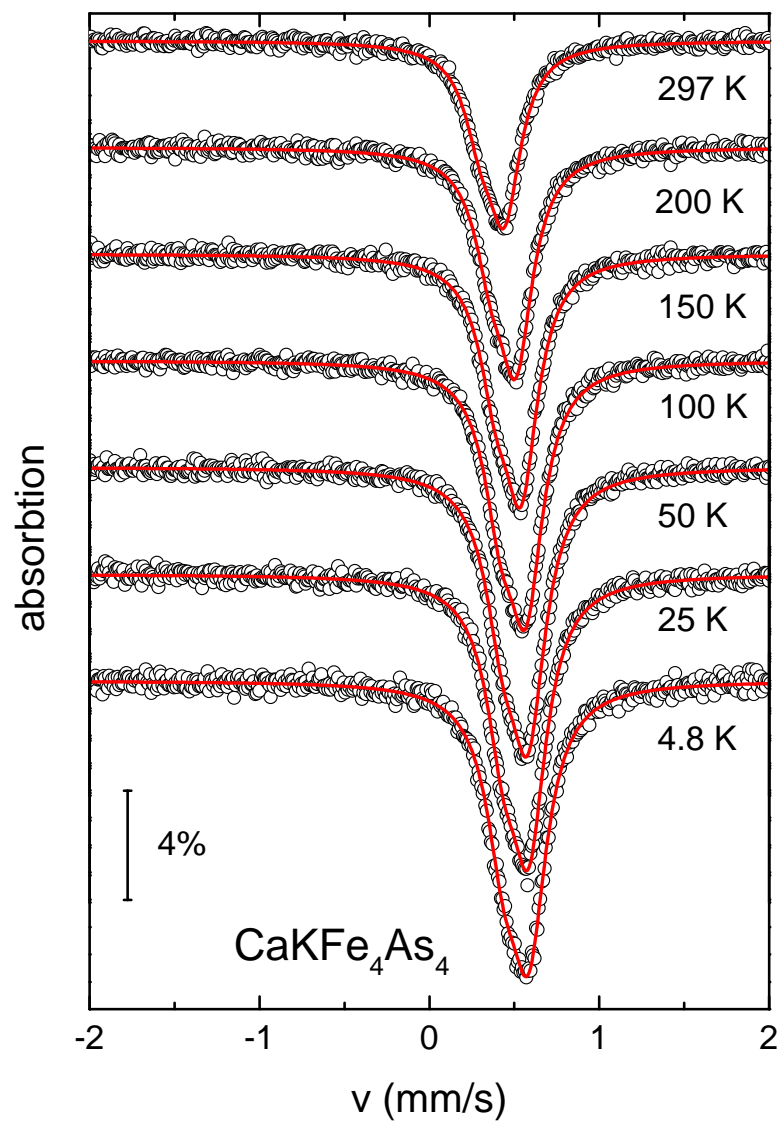


Figure 3: (Color online) ^{57}Fe Mossbauer spectra of $\text{CaKFe}_4\text{As}_4$ at selected temperatures. Symbols-data, lines-fits.

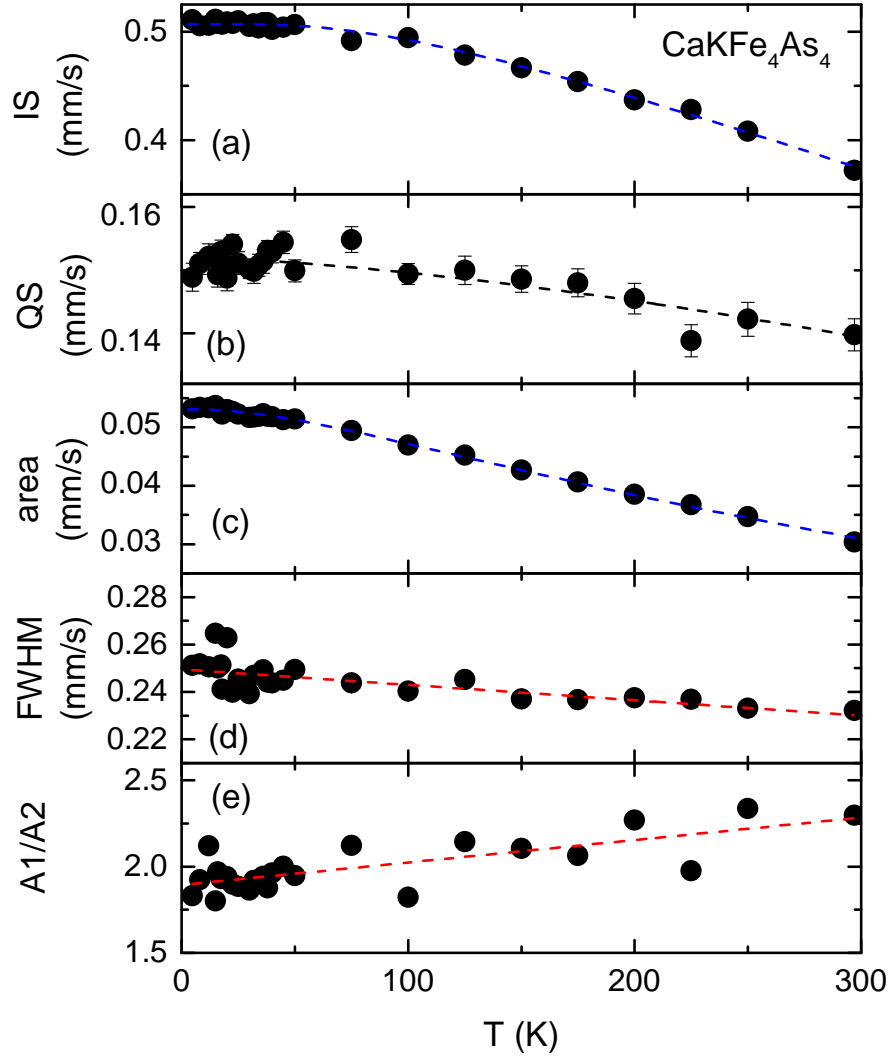


Figure 4: (Color online) Temperature dependencies of the hyperfine parameters obtained from fits of ^{57}Fe Mossbauer spectra of $\text{CaKFe}_4\text{As}_4$ at different temperatures: (a) isomer shift, (b) quadrupole splitting, (c) area normalized to the baseline, (d) linewidth (full width at half maximum), and (e) intensity ratio of the doublet lines. Symbols: data, lines (a), (c) Debye fits (see text), (b) “ $T^{3/2}$ law” (see text), (d), (e) linear fits that serve as guide to the eye.

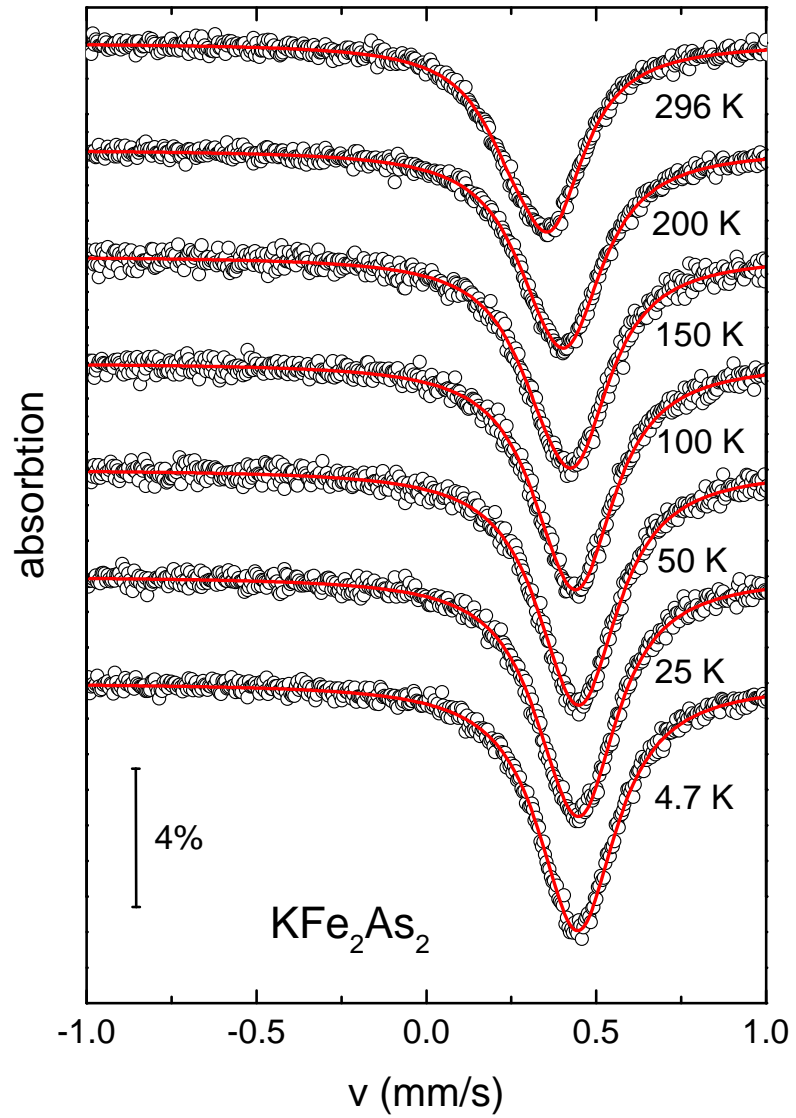


Figure 5: (Color online) ^{57}Fe Mossbauer spectra of KFe_2As_2 at selected temperatures. Symbols-data, lines-fits.

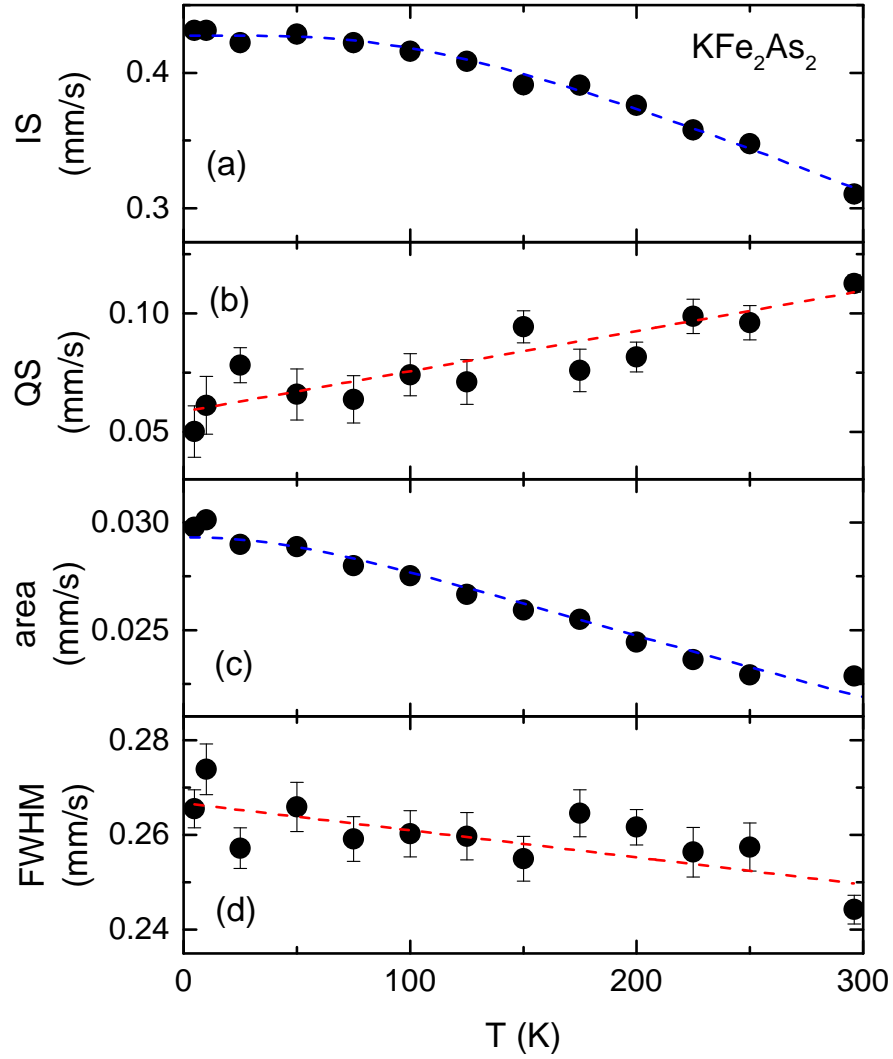


Figure 6: (Color online) Temperature dependencies of the hyperfine parameters obtained from fits of ^{57}Fe Mossbauer spectra of KFe_2As_2 at different temperatures: (a) isomer shift, (b) quadrupole splitting, (c) area normalized to the baseline, (d) linewidth (full width at half maximum). Symbols: data, lines (a), (c) Debye fits (see text), (b) and (d) linear fits that serve as guide to the eye.

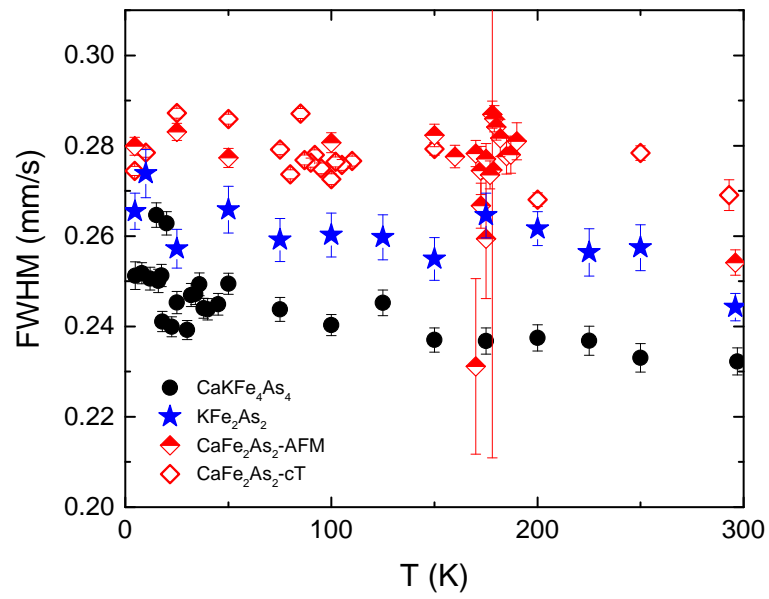


Figure 7: (Color online) Temperature dependencies of the linewidth (full width at half maximum) obtained from fits of ^{57}Fe Mossbauer spectra of $\text{CaKFe}_4\text{As}_4$, KFe_2As_2 (this work) and CaFe_2As_2 [14, 24] at different temperatures.

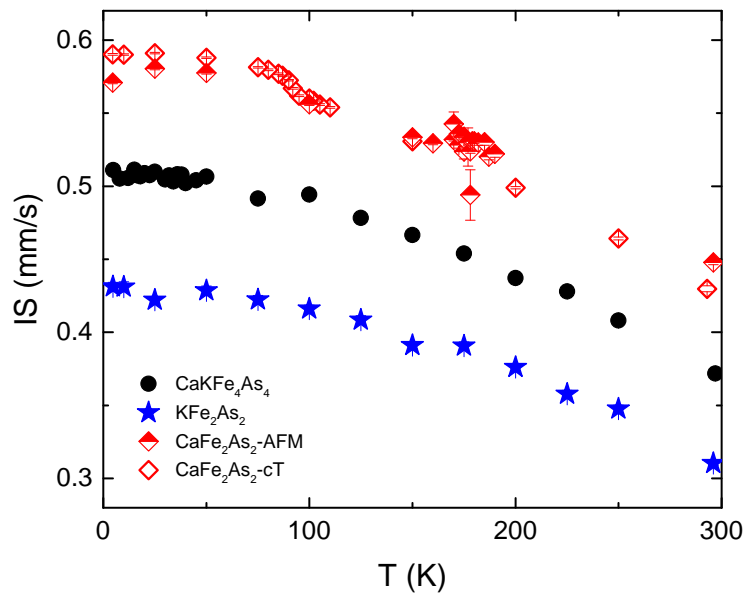


Figure 8: (Color online) Temperature dependencies of the isomer shift obtained from fits of ^{57}Fe Mossbauer spectra of $\text{CaKFe}_4\text{As}_4$, KFe_2As_2 (this work) and CaFe_2As_2 [14, 24] at different temperatures.

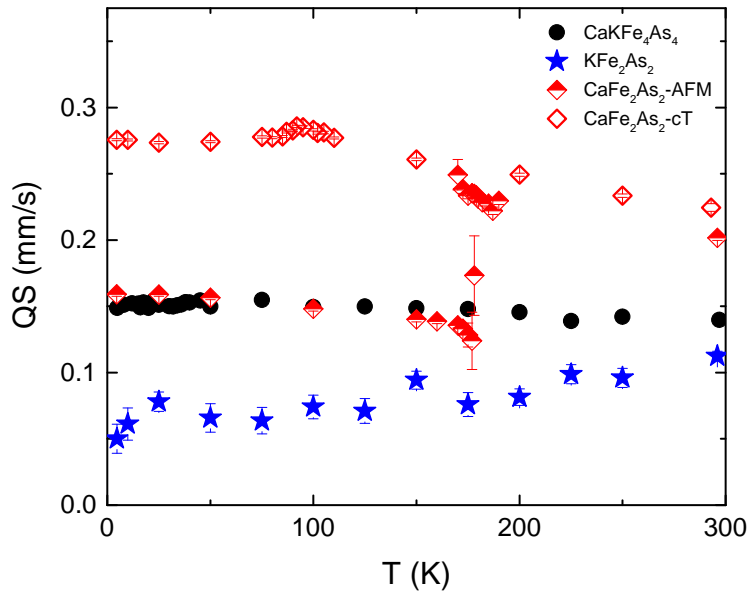


Figure 9: (Color online) Temperature dependencies of the quadrupole splitting obtained from fits of ^{57}Fe Mossbauer spectra of $\text{CaKFe}_4\text{As}_4$, KFe_2As_2 (this work) and CaFe_2As_2 [14, 24] at different temperatures. Note that for CaFe_2As_2 - AFM the absolute values of the quadrupole splitting are plotted in the magnetically ordered state.

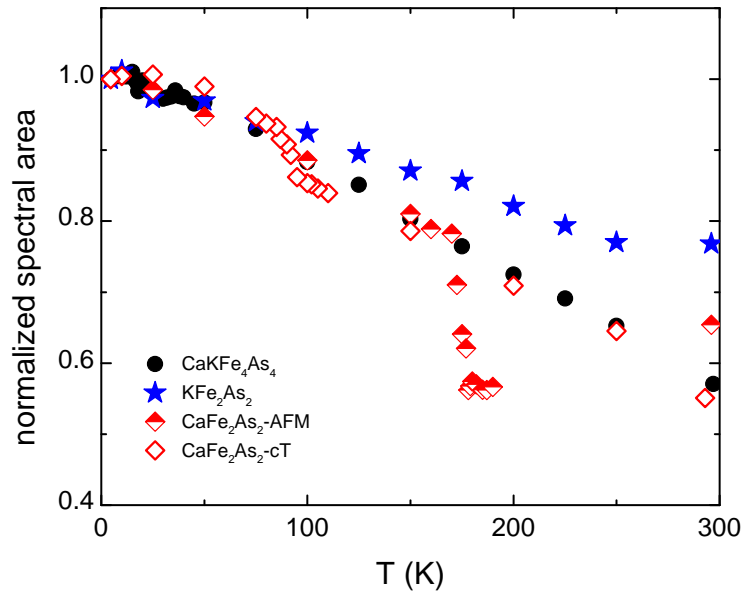


Figure 10: (Color online) Temperature dependencies of the spectral area normalized to the corresponding value at the base temperature (4.6 K - 4.8 K) obtained from fits of ^{57}Fe Mossbauer spectra of $\text{CaKFe}_4\text{As}_4$, KFe_2As_2 (this work) and CaFe_2As_2 [14, 24] at different temperatures.